

Learning to Reconstruct: A Differentiable Approach to Muon Tracking at the LHC

Andrea Coccaro¹, Francesco Armando Di Bello^{2,3}, Lucrezia Rambelli^{1,4}, Stefano Rosati⁵, Carlo Schiavi^{1,4}

¹INFN, Sezione di Genova, 16146 Genova, Italy.

²Department of Physics, Università di Pisa, 56127 Pisa, Italy.

³INFN, Sezione di Pisa, 56127 Pisa, Italy.

⁴Department of Physics, Università di Genova, 16146 Genova, Italy.

⁵INFN, Sezione di Roma, 00185 Rome, Italy.

Abstract

Reconstructing the trajectories of charged particles in high-energy collisions requires high precision to ensure reliable event reconstruction and accurate downstream physics analyses. In particular, both precise hit selection and transverse momentum estimation are essential to improve the overall resolution of reconstructed physics observables. Enhanced momentum resolution also enables more efficient trigger threshold settings, leading to more effective data selection within the given data acquisition constraints. In this paper, we introduce a novel end-to-end tracking approach that employs the differentiable programming paradigm to incorporate physics priors directly into a machine learning model. This results in an optimized pipeline capable of simultaneously reconstructing tracks and accurately determining their transverse momenta. The model combines a graph attention network with differentiable clustering and fitting routines, and is trained using a composite loss that, due to its differentiable design, allows physical constraints to be back-propagated effectively through both the neural network and the fitting procedures. This proof of concept shows that introducing differentiable connections within the reconstruction process improves overall performance compared to an equivalent factorized and more standard-like approach, highlighting the potential of integrating physics information through differentiable programming.

Keywords: high-energy physics, track reconstruction, machine learning, differentiable programming

1 Introduction

Track reconstruction is a fundamental task in particle-physics experiments, as it provides key observables – particle trajectories, momenta and vertex information – essential for physics analyses. Traditional tracking approaches in High Energy Physics rely on a factorized pipeline, where pattern recognition and track fitting are treated, and optimized, as separate steps. With the forthcoming increase in luminosity and data complexity at the LHC [1], developing optimized methods for tracking has become an important research direction [2, 3], also considering the important detector upgrades of the ATLAS and CMS collaborations [4, 5].

Furthermore, recent interesting developments have focused on integrating physics information into machine learning models to improve their accuracy, with differentiable programming techniques proving to be highly effective for implementing these priors [6–9].

In this context, we designed and implemented a novel machine-learning based model which represents an end-to-end, differentiable approach to track reconstruction. To demonstrate the effectiveness of the proposed technique, we focus, as a concrete use case, on single muon track reconstruction of a typical LHC experiment [10, 11], restricting the problem on the 2D plane containing the particle’s trajectory.

Traditional tracking methods typically rely on a sequence of separate, factorized steps. In particular using as inputs the hits registered by the detector by the traversing particles a clustering procedure and, subsequently, a fit procedure is applied to accurately determine the particle’s transverse momentum (p_T).

Unlike such traditional methods, the proposed model, thanks to the definition of differentiable blocks which allows to have a physics-informed weight backpropagation, directly maps raw detector hits to the particle’s transverse momentum within a single integrated pipeline. The model is based on a Graph Attention Network (GAT) [12], representing detector hits as graph nodes and exploiting their spatial correlations to identify those associated with a single muon trajectory. Clustering and fitting operations are embedded as differentiable modules, allowing the entire process, from hit classification to momentum estimation, to be jointly optimized through backpropagation. This design makes the reconstruction inherently physics-informed and capable of learning the track curvature directly from the data. The model is developed in a JAX-based environment [13], which provides automatic differentiation, just-in-time compilation, and vectorization, ensuring both flexibility and computational efficiency. Applied to a toy simulation based on the ATLAS muon-spectrometer geometry and noise, the model demonstrates promising results in both hit classification and transverse momentum estimation and outperforms a sequential baseline approach. These achievements show the potential of differentiable, end-to-end techniques to become an alternative to traditional tracking algorithms.

2 Detector simulation

In order to develop the benchmark models considered in this study, a MC simulation of a tracking detector has been designed.

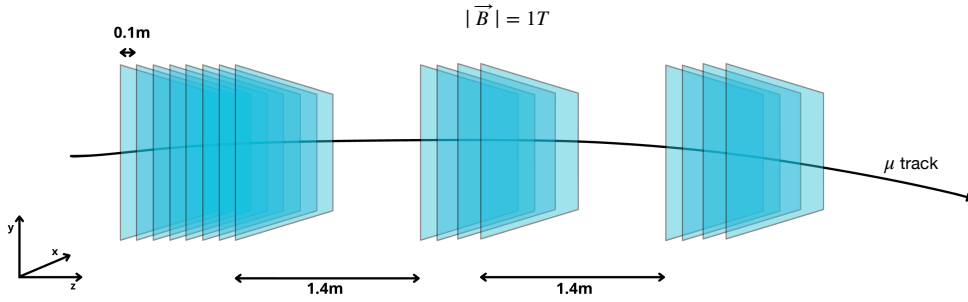


Fig. 1: Layout of the detector geometry simulated in the toy model

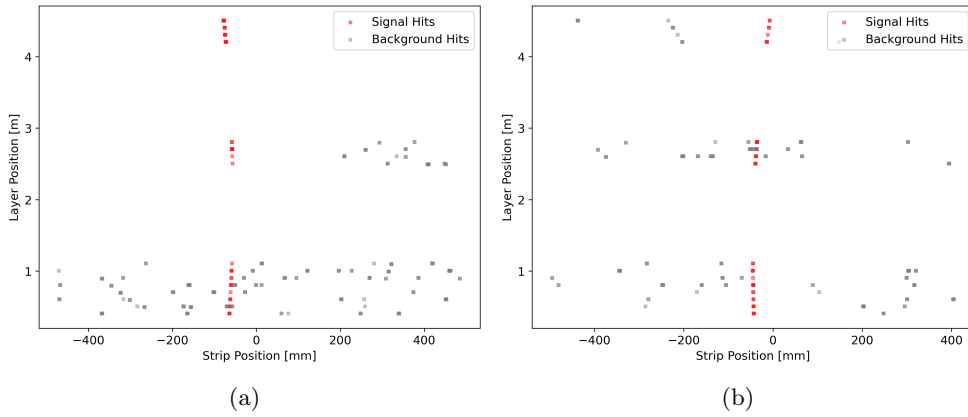


Fig. 2: Two examples of event displays, both showing the track originating from the muon particle and additional activity related to both detector noise and secondary tracks.

The detector layout, depicted in Figure 1, is composed by 16 tracking layers, divided into three stations. The first station has 8 layers each, while the other two stations have 4 layers each. The detector is immersed in a 1 T uniform magnetic field directed along the x -axis, as depicted in the figure. The simulation of this layout has been realized with GEANT4 [14], assuming that each detector layer is composed by two printed circuit boards with a 1 cm thickness, interleaved with a sensitive gap of 5 mm and a strip pitch of 0.5 mm. This layout is inspired by micro-pattern gaseous

detectors used in the LHC experiments, such as the MicroMegas [15] or the GEM [16] detectors, and in particular by the design of the Phase-I ATLAS muon upgrade [17].

The detector response is simulated by extrapolating the particle trajectories to the readout planes, and getting the hit position on each plane. A cluster of firing strips is built around the position of the hit, with an average cluster size of 4 strips. The charge per strip is generated according to a gaussian distribution, centered in the hit position with a sigma corresponding to 2/3 of the strip pitch. This ensures that a charge always very close to the full cluster charge is contained within the cluster. If two or more hits generate overlapping clusters, the charge contributions are summed over all clusters, for each readout channel in the overlap region.

The simulated sample is composed of single muons events with a transverse momentum in the range [20, 50] GeV. Examples of event displays, with hits from signal tracks and from both noise or additional scattering tracks, are depicted in Figure 2.

3 Model

Tracking, the task of reconstructing particle candidates from a set of detector hits x , is composed of several algorithmic stages. Considering as input variables the geometrical coordinates in the yz -plane of each detector hit, the reconstructed transverse momentum of the particle \hat{p}_ϕ is obtained as

$$\hat{p}_\phi = f_{\chi^2\text{-min}} \circ f_{\text{clustering}} \circ f_\phi(x).$$

As outlined in the above equation, the entire processing chain is differentiable, allowing end-to-end optimization of \hat{p}_ϕ through gradient-based learning.

The function f_ϕ represents the pattern recognition module, implemented as a GAT with trainable parameters ϕ . It receives detector signals as input and outputs a set of weights w_i , corresponding to the probability that the i -th hit was produced by a signal muon. More details on the actual architecture of the GAT are presented in Appendix A.

Using as input the predicted weights for each graph node and the original features representing the spatial coordinates, the clustering module, $f_{\text{clustering}}$, computes the muon position \bar{y}_j in each detector layer j as a weighted average of hit positions:

$$\bar{y}_j = \frac{\sum_{i \in j} w_i y_i}{\sum_{i \in j} w_i},$$

where \bar{y}_j denotes the reconstructed muon position in layer j .

The RMS of the detector hits associated with the muon in that layer is used as the positional uncertainty $\sigma_{\bar{y}_j}$. An additional weight \mathbf{W}_j is then associated to each cluster and defined as the sum of all the predicted weights w_i for the hits in the given layer j used for the cluster position definition.

The χ^2 minimization stage $f_{\chi^2\text{-min}}$ implements the fitting procedure using as input the reconstructed positions \bar{y}_j and a matrix inversion procedure based on the Kasa method [18]. Layer-wise weights, defined as $\mathbf{W}_j/\sigma_{\bar{y}_j}^2$, are incorporated in each matrix

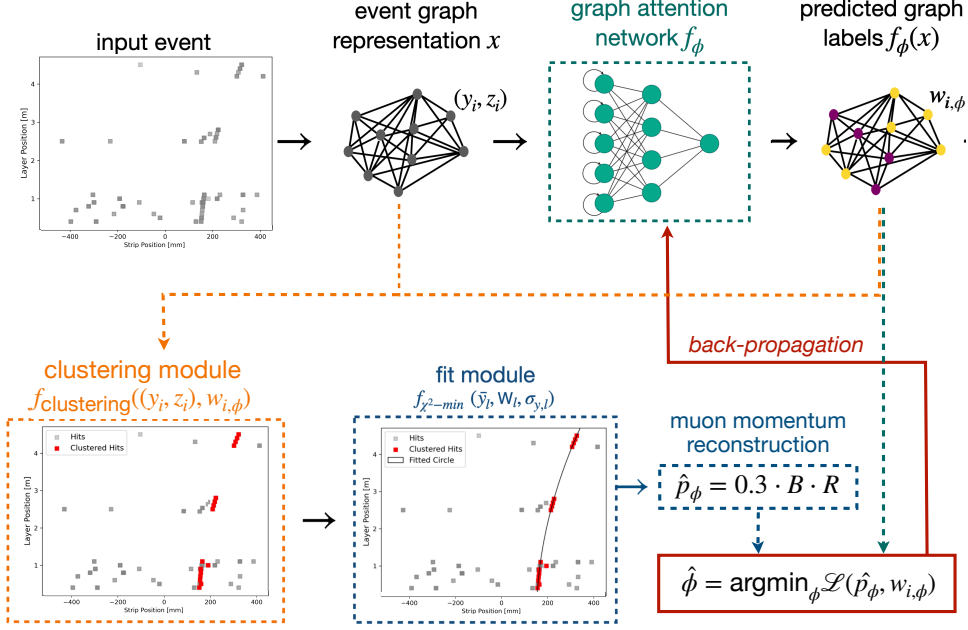


Fig. 3: Schematic representation of the end-to-end model developed for track reconstruction. Both the clustering and fitting routines depend on the GAT learnable parameters through the predicted node labels $w_{i,\phi}$. The regression of the particle’s p_T is back-propagated to the pattern recognition module as visualized in the figure and described in more details within the text.

element. The corresponding output is the reconstructed muon momentum \hat{p}_ϕ through the relation $\hat{p}_\phi = 0.3 B r$ and with r the fitted radius.

The network trainable parameters are determined by minimizing the following composite loss function:

$$\begin{aligned} \hat{\phi} &= \arg \min_{\phi} \mathcal{L}(\hat{p}_\phi, w_{i,\phi}) = \\ &= \arg \min_{\phi} \sum_{\text{events}} \left[\alpha \frac{(\hat{p}_\phi - p)^2}{p^2} + \frac{1}{N_{\text{hits}}} \sum_{i=1}^{N_{\text{hits}}} \text{BCE}(w_{i,\phi}, y_{i,\text{truth}}) \right]. \end{aligned}$$

This loss function consists of two distinct components, targeting both hits classification and momentum regression tasks. Here, the momentum p in the loss term reflects the true p_T value for each event, while $y_{i,\text{truth}}$ designates the truth labels corresponding to each individual node within the graph. The hyperparameter α balances the regression and classification components and it is empirically set to 0.5. During the early training epochs, α is set to 0 so that only the binary cross-entropy (BCE) term is initially

considered. This two-stage approach was observed to yield a more rapid convergence of the training process.

The model is trained on a dataset of 10^4 events, while evaluation is performed on an independent test sample of 9k events. Optimization was performed using Adam [19], with an OPTAX scheduler [20] that gradually decays the learning rate.

4 Results

The performance of the proposed end-to-end model is evaluated using two complementary criteria: hit-classification accuracy and reconstructed p_T resolution. These metrics assess the model’s ability to discriminate signal hits from background noise and to accurately reconstruct particle kinematics.

The performance is compared to what is obtained by another model with the same architecture but trained solely for the node classification task, hence by setting $\alpha = 0$ in the composite loss function. This approach mimics the standard sequential workflow for tracking, in which hit classification and trajectory reconstruction are factorized and executed independently. In particular the p_T reconstruction is done applying the clustering and circle-fitting steps using the same definitions and weighting schemes used for the main model, but outside of the end-to-end pipeline. Throughout the subsequent discussion and figures, these two models are referred to as the end-to-end and baseline models.

For the classification task, performance is evaluated by constructing score histograms for true signal and background hits, and by generating a receiver operating characteristic (ROC) curve through threshold scanning over the predicted scores. The resulting plot, depicted in Figure 4, shows how including the p_T loss term improves classification performance and demonstrates that the differentiable end-to-end coupling of the physics-driven p_T objective greatly benefits the node-level predictions.

A complementary study was performed to assess the spatial resolution of the reconstructed cluster positions. The analysis examines the residual distributions between the reconstructed cluster coordinates and the truth muon impact point on each detector layer. Residual distributions were evaluated for three configurations: the idealized truth-weighted clustering, the baseline model, and the proposed end-to-end model. Using a Gaussian fit to the truth distribution to define the detector’s core resolution window, we measure the fraction of clusters with residuals within this region. The end-to-end model increases this fraction by 12.7% relative to the baseline, demonstrating a clear improvement in spatial reconstruction performance.

In a similar fashion, the reconstructed p_T accuracy is compared across these three different methodologies for assessing the impact of the end-to-end training approach. The reconstructed p_T is evaluated by analyzing the q/p_T residual distributions, with q being the muon charge. Figure 5 shows these distributions for the three approaches. Following the procedure outlined in Reference [21], a width σ^* , defined as half the interval, centered around the median of the distribution and that contains 68% of events, is calculated. The σ^* distributions for the three cases are presented in Figure 5,

which demonstrates a clear improvement in p_T resolution for the end-to-end model relative to the sequential baseline.

We further study the residuals in the reconstructed p_T and in 5-GeV bins across the 20–50 GeV range. In this case the truth p_T value associated to each muon in the sample is used as a comparison, and the binned σ^* vs. p_T trend is computed again with using the truth labels as weights in the procedure and with the predictions from both the baseline and the end-to-end models. As clearly visible in Figure 6, across all bins the end-to-end approach yields systematically smaller σ^* values, demonstrating improved resolution from incorporating the differentiable p_T term in the training.

5 Conclusions

In this work, we introduced a novel end-to-end tracking approach that incorporates differentiable programming techniques to embed physics information directly into the training of a machine-learning model.

The proposed model demonstrates a notable performance enhancement with respect to a more traditional approach where hit classification and fitting procedures are two sub-sequent and factorized steps of the reconstruction. Specifically, the ROC

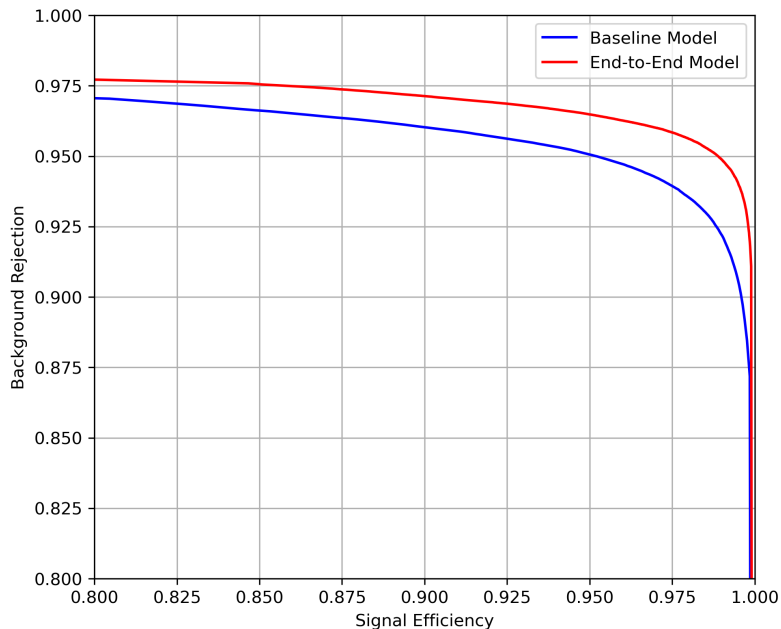


Fig. 4: ROC distributions for the hit classification task for both the baseline and the end-to-end models for tracking. The end-to-end model directly incorporates physics priors and perform simultaneously both the hit classification and the transverse-momentum regression. The performance clearly shows how the end-to-end approach boosts the accuracy of the hit classification task.

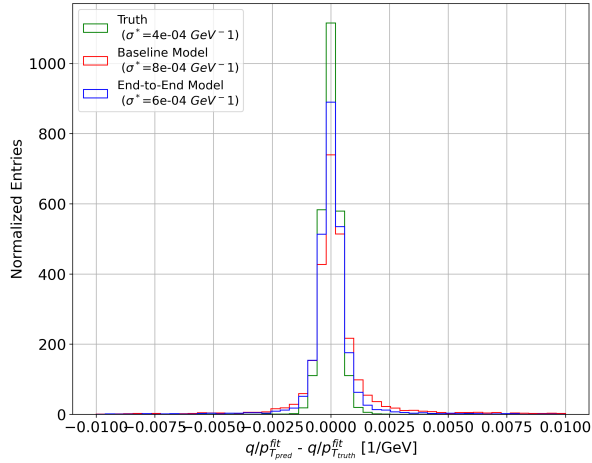


Fig. 5: Normalized q/p_T residual distributions, with q being the charge of the reconstructed muon. The three distributions correspond to using the truth labels as input weights in the clustering step, using the baseline model predictions and those from the proposed end-to-end model. The end-to-end model demonstrates improved accuracy in p_T regression, approaching the limit of an ideal detector.

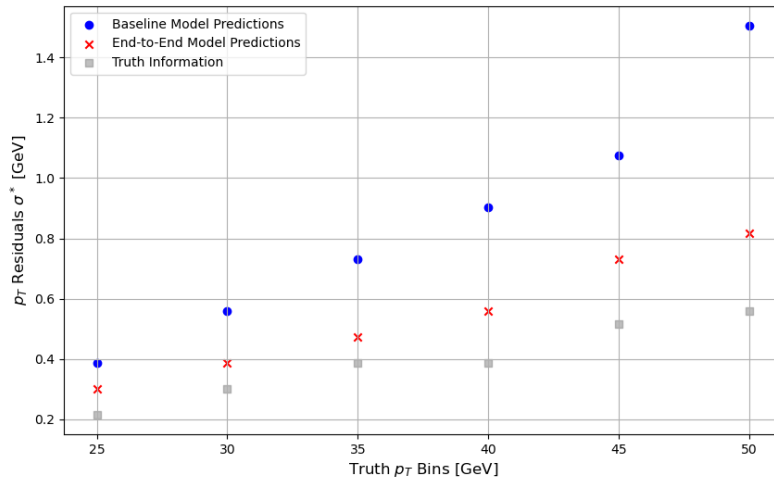


Fig. 6: p_T residual distributions as a function of the truth p_T values

curve in Figure 4 shows how the end-to-end training yields a consistently higher background rejection at equivalent signal efficiencies for classifying detector hits. This demonstrates that integrating a physics-aware contribution within the loss function, particularly for regressing the muon p_T , enhances the model discriminative capabilities

beyond what classification alone can achieve. This is made possible by the differentiable formulation of clustering and fitting functions used for the p_T computation.

Overall, the combined evidence from ROC metrics and residual distributions consistently supports the advantages of the end-to-end, differentiable design. By embedding physics constraints into the training process, the end-to-end approach delivers improved hit classification accuracy and produces reconstructed clusters that more faithfully reflect true particle paths.

6 Acknowledgments

We thank the IT team of the INFN Rome section and Physics department at La Sapienza university, and in particular Francesco Safai Tehrani for the useful support in accessing the local GPU computing infrastructure. The authors are also grateful to Michael Kagan and Lukas Henrich for inspiring discussions.

A Model Architecture

The differentiable end-to-end model is based on two stacked neural networks inspired by the Graph Attention Network (GAT). The initial graph is built as fully connected using the recorded hits as input nodes.

The node embedding is computed via an MLP which maps the input features \mathbf{x}_i of each node i into a hidden representation of dimension 512:

$$\mathbf{q}_i = \text{attention_query}(\mathbf{x}_i) \in \mathbb{R}^{512}.$$

The raw attention logit is computed as an edge feature:

$$\mathbf{e}_{ij} = \text{attention_logit}(\mathbf{q}_i, \mathbf{q}_j) \in \mathbb{R}^{512},$$

where, to increase the expressivity of the network, \mathbf{e}_{ij} is a vector-valued attention score of dimension 512. A dimension-wise softmax normalization is applied over all incoming edges of each receiving node:

$$\alpha_{ij}^{(d)} = \frac{\exp(e_{ij}^{(d)})}{\sum_{k \in \mathcal{N}(j)} \exp(e_{kj}^{(d)})}, \quad d = 1, \dots, 512,$$

where $\mathcal{N}(j)$ denotes the neighbors of node j . The updated node features are computed via element-wise multiplication and aggregation:

$$\mathbf{h}'_j = \sum_{i \in \mathcal{N}(j)} \alpha_{ij} \odot \mathbf{q}_i,$$

where \odot denotes the Hadamard product and $\alpha_{ij} = [\alpha_{ij}^{(1)}, \dots, \alpha_{ij}^{(512)}]^\top$.

The second GAT layer uses the output \mathbf{h}'_j from the first layer as input. The attention mechanism is identical to the first layer, but includes an additional node update function that compresses the 512-dimensional representation to a scalar via an MLP followed by sigmoid activation:

$$\mathbf{h}''_j = \sigma \left(\text{node_update} \left(\sum_{i \in \mathcal{N}(j)} \alpha_{ij} \odot \mathbf{h}'_i \right) \right) \in [0, 1],$$

where σ is the sigmoid function. Table 1 summarizes the implementation details of both GAT layers.

Stage	Description
Input graph	Nodes: (y, z) coordinates of hits Edges: fully connected graph with self-edges
GAT layer 1	Attention query: MLP([4, 8, 16, 32, 64, 128, 256, 512]) Attention logit: MLP([1024, 512] \rightarrow [512]) + LeakyReLU
GAT layer 2	Attention query: Identity Attention logit: MLP([1024, 512] \rightarrow [512]) + LeakyReLU Node update: MLP([512, 256, 128, 64, 32, 16, 8, 4, 2, 1]) + Sigmoid

Table 1: Details of the implementation of the GAT layers used for the end-to-end architecture for the task of muon tracking.

References

- [1] O. Aberle, *et al.*, High-Luminosity Large Hadron Collider (HL-LHC): Technical design report, CERN-2020-010 (2020).
- [2] J. Shlomi, P. Battaglia and J. R. Vlimant, Graph Neural Networks in Particle Physics, arXiv 2007.13681.
- [3] H. Zhao, *et al.*, Track reconstruction as a service for collider physics, JINST **20** (2025) no.06, P06002.
- [4] ATLAS Collaboration, The ATLAS Experiment at the CERN Large Hadron Collider, JINST **3** 2008, S08003.
- [5] CMS Collaboration, The CMS experiment at the CERN LHC, JINST **3**(2008), S08004.
- [6] P. De Castro and T. Dorigo, INFERNO: Inference-Aware Neural Optimisation, Comput. Phys. Commun. **244** (2019), 170-179.
- [7] N. Simpson and L. Heinrich, Neos: End-to-End-Optimised Summary Statistics for High Energy Physics, J. Phys.: Conf. Ser. **2438** (2023) no.1, 012105.
- [8] M. Vigl, N. Hartman and L. Heinrich, Finetuning foundation models for joint analysis optimization in High Energy Physics, Mach. Learn. Sci. Tech. **5** (2024) no.2, 025075.
- [9] R. E. C. Smith, I. Ochoa, R. Inácio, J. Shoemaker and M. Kagan, Differentiable vertex fitting for jet flavor tagging, Phys. Rev. D **110** (2024) no.5, 052010.
- [10] ATLAS Collaboration, Muon reconstruction and identification efficiency in ATLAS using the full Run 2 pp collision data set at $\sqrt{s} = 13$ TeV, Eur. Phys. J. C **81** (2021) no.7, 578.
- [11] CMS Collaboration, Performance of the CMS muon detector and muon reconstruction with proton-proton collisions at $\sqrt{s} = 13$ TeV, JINST **13** (2018) no.06, P06015.

- [12] P. Veličković, *et al.*, Graph Attention Networks, arXiv 1710.10903.
- [13] J. Bradbury, *et al.*, JAX: composable transformations of Python+NumPy programs, <http://github.com/jax-ml/jax>.
- [14] S. Agostinelli et al., GEANT4 - A Simulation Toolkit, Nucl. Instrum. Meth. A **506** (2003) 250.
- [15] Y. Giomataris, P. Rebourgeard, J. Robert, and G. Charpak, MICROMEGAS: A High granularity position sensitive gaseous detector for high particle flux environments, Nucl. Instrum. Meth. A **376** (1996) 29-35.
- [16] F. Sauli, GEM: A new concept for electron amplification in gas detectors, Nucl. Instrum. Meth. A **386** (1997), 531-534.
- [17] T. Alexopoulos, *et al.*, Construction techniques and performances of a full-size prototype Micromegas chamber for the ATLAS muon spectrometer upgrade, Nucl. Instrum. Meth. A **955** (2020) 162086.
- [18] I. Kasa, A curve fitting procedure and its error analysis. IEEE Transactions on Instrumentation and Measurement, 25 (1976), 1, 8–14.
- [19] D. P. Kingma, J. Ba, Adam: A Method for Stochastic Optimization, International Conference on Learning Representations (ICLR), arXiv:1412.6980.
- [20] DeepMind, The DeepMind JAX Ecosystem, <https://github.com/deepmind/optax>.
- [21] ATLAS Collaboration, Studies of the muon momentum calibration and performance of the ATLAS detector with pp collisions at $\sqrt{s} = 13$ TeV, Eur. Phys. J. C **83** (2023) no.8, 686.